International Journal of Innovative Computing, Information and Control
Volume **21**, Number **1**, February **2025**

 ISSN 1349-4198
pp. **53–67**

NEWLY PROPOSED METHOD OF PRESSURE MEASUREMENT BY TRACKING PARTICLES FOR UNDERWATER MICRO SHOCK WAVES

Ayumu Yamamoto and Masaaki Tamagawa*

Graduate School of Life Science and Systems Engineering
Kyushu Institute of Technology
2-4, Hibikino, Wakamatsu-ku, Kitakyushu, Fukuoka 808-0196, Japan
yamamoto.ayumu226@mail.kyutech.jp; *Corresponding author: tama@life.kyutech.ac.jp

Received April 2024; revised August 2024

Abstract. *This paper describes a novel method for pressure measurements of underwater micro shock waves induced by pulse laser. The underwater shock waves are measured by a hydrophone in general. However, it is difficult to measure the pressure of the micro shock wave accurately because its active area is smaller than the sensitive area of the hydrophone. This research proposed methods applying particle tracking velocimetry as the measurement for the micro shock waves. The pressure of the shock wave was calculated from two types of calculation processes with different hypotheses for the change of particle velocity. Method 1 assumed that the velocity of the particle receiving the shock waves decelerates exponentially, and method 2 assumed that the velocity decelerates linearly. As the result of method 1, the pressure at the laser-focal area was calculated to be 28.92 MPa which was higher than the pressure estimated from results measured by hydrophone. Conversely, the pressure at the laser-focal area was calculated to be 7.02 MPa from method 2, which was in the same order as the estimated pressure. From these experiments, it was possible that the proposed pressure measurement applying PTV could be applied to the measurement pressure of micro shock waves.*

Keywords: Pressure measurement, Particle tracking velocimetry, Laser-induced underwater micro shock wave, Femtosecond laser

1. **Introduction.** Recently, the effects of mechanical stimulations using shock waves on organisms and cells have been studied [1-3]. As the stimulation for individual cells, using the micro shock waves has been expected [4-6]. The micro shock waves can be generated by focusing a short pulse laser to water [7-20]. It is important to investigate the pressure distributions of the micro shock waves to understand the effects of stimulation on the cells. In general pressure of underwater shock waves is measured using a hydrophone [10]. However, it is difficult to measure the pressure of the micro shock wave accurately because its active area is smaller than the sensitive area of the hydrophone. In other ways, Vogel et al. have calculated the pressure of the micro shock waves induced by nanosecond pulse laser from the propagation velocity of shock wave front taken by photography [12]. As the method using photography, Hayasaka et al. have reported that the micro shock waves can be quantified by applying the BOS (background-oriented schlieren) technique [9]. However, a highly expensive setup is needed in these methods because it includes a camera capable of high time resolution. Conversely, Iino and Hosokawa have evaluated the pressure of the micro shock waves by applying atomic force microscopy, although it is unsuitable for measurement of high-speed phenomena because of low-frequency bandwidth [18].

DOI: 10.24507/ijicic.21.01.53

In this research, novel methods applying particle tracking velocimetry were proposed as the measurement for the micro shock waves. The proposed measurement is expected to be cost-effective to implement by using the particles smaller than the effective area of the micro shock waves, and a normal camera which is not expensive. The micro shock waves were generated by focusing a femtosecond pulse laser to water which includes particles, and the pressure of shock waves was calculated from the moving velocity of particles received shock waves. In this method, the pressure calculated from two types of processes with different hypotheses for change in particle velocity; method 1 was assumed that the velocity of the particle receiving the shock waves decelerates exponentially, and method 2 was assumed that the velocity decelerates linearly. Furthermore, results obtained from both methods were compared with the pressure measured using a hydrophone.

2. Pressure Measurement of Micro Shock Waves through Hydrophone.

2.1. Femtosecond laser-induced underwater micro shock wave generator and experimental setup. Figure 1 shows a schematic of the femtosecond laser-induced underwater micro shock wave generator. The laser was irradiated from a femtosecond (pulse) laser device (EKSPLA, FF3000, wavelength 1030 nm, pulse duration time 260 fs, pulse energy 2.1 μJ) and the beam direction was changed to 90° downward by a hot mirror. The laser was focused on a depth of 1 mm in distilled water (Takasugi Pharmaceutical Co., Ltd.) by an objective lens (Mitutoyo Corporation, M PLAN APO NIR 100X, NA 0.5, convergence angle 30° (22° in water)). The real depth became 1.43 mm by influence of refractive index of water. The repetition frequency of the laser was controlled to 1 Hz by the function generator.

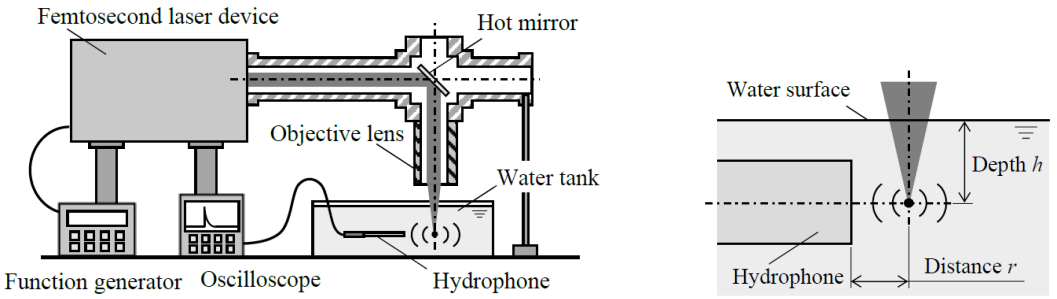

(a) Overall view of experimental setup (b) Enlarged view at laser-focal area

FIGURE 1. Laser-induced micro shock wave generator and the position of hydrophone

The radius of the laser-focal area δ is typically obtained as follows [15]:

$$\delta = 0.61\frac{\lambda}{\mathrm{NA}}, \tag{1}$$

where, λ is the wavelength of the laser and NA is the numerical aperture of the objective lens. From the specification, λ was fixed at 1030 nm and NA was fixed at 0.5. The radius δ was calculated to be 1.257 μm in this experiment from Equation (1).

The pressure of the micro shock waves was measured using a hydrophone (Müeller Instrument, Müeller-Platte Needle Probe, sensitive diameter 0.5 mm, rise time 40 ns), and recorded using an oscilloscope (Yokogawa Test & Measurement Corporation, DL1740, sampling rate 500 MHz, bandwidth 400 MHz) as a waveform. As shown in Figure 1(b), measurement distance r was defined as the horizontal distance from the laser-focal area to the hydrophone. In this experiment, r was changed from 300 μm to 1000 μm in 100

μm steps. Here, the minimum distance was determined to 300 μm because any contact between the laser and the hydrophone was avoided. These measurements were conducted 20 times at each distance.

2.2. **Pressure history of micro shock waves.** Figure 2 shows a typical pressure history of the micro shock wave at $r = 300$ μm. From Figure 2, it was observed that the peak pressure of micro shock waves was approximately 0.4 MPa at $r = 300$ μm. Next, the peak pressure at the laser-focal area was estimated by the measured peak pressure at each distance. The peak pressure at any distance $P(r)$ is approximated by Equation (2) as equation of extrapolation,

$$P(r) = \frac{\beta}{r^{\alpha}}, \tag{2}$$

where, α and β are constants determined by applying the least square method to the experimental result.

Figure 3 shows a peak pressure at each measurement distance and the estimated pressure at the laser-focal area. In Figure 3, each black plot is the averaged peak pressure, the dotted line is the extrapolation curve, and the white plot is the estimated pressure at the laser-focal area. From Equation (1) and Equation (2), the peak pressure at the laser-focal

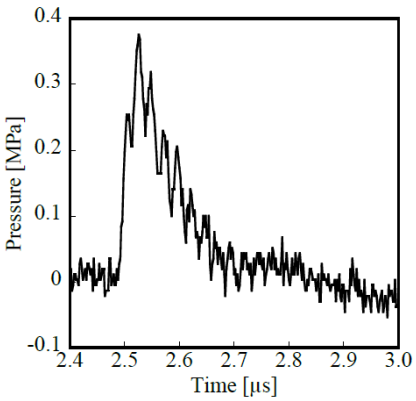

FIGURE 2. Pressure history of micro shock wave at 300 μm

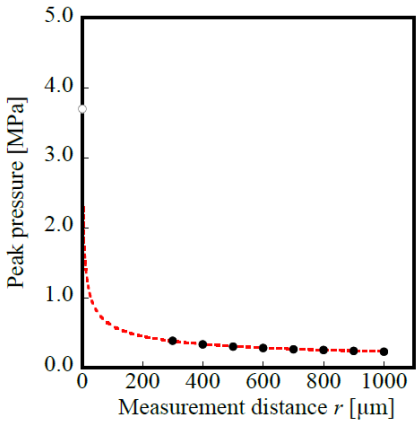

(a) Peak pressure at each distance and estimated pressure at laser-focal area

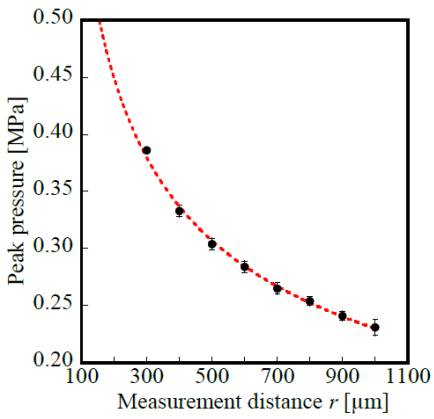

(b) Enlarged view of peak pressure at each distance (Error bar shows 95% confidence interval)

FIGURE 3. Result of measuring micro shock wave pressure by pressure sensor

area was calculated as the pressure at $\delta = 1.257$ μm. As a result, the peak pressure at the laser-focal area was estimated to be 3.70 MPa when constants α and β were 0.416 and 4.07 MPa, respectively. Although it has been reported that α was approximately 1 in the case of the spherical shock waves [7,10], obtained α in this experiment was about 0.4 which indicates more gradual than other's results. As the reason, it was considered that the pressure was not measured at the distance where the pressure attenuates rapidly around $r = 0 \sim 100$ μm. In this experiment, the diameter of the hydrophone and the minimum measurement distance were over 100 times of the laser-focal area. However, it was difficult to measure any closer to avoid any contact between the laser and the hydrophone. Therefore, there is suspicion that the estimation method for this experiment has poor accuracy. In this distance under 100 μm, it is anticipated that the affective area of shock waves is small, and its velocity is extremely high. It was considered that a direct measurement method is needed to obtain more accurate pressure at the laser-focal area. In the next section, pressure measurements applying PTV as a more direct method is mentioned.

3. Method 1 of Pressure Measurement Applying PTV.

3.1. **Experimental setup for method 1.** Figure 4 shows the flowchart of process to obtain shock wave pressure on method 1. As shown in Figure 4, first, images of moving particles received shock waves are obtained, and the velocity of particles is calculated. Next, the pressure of shock waves is calculated from the velocity. In this section, the experimental setup is mentioned. Figure 5 shows a schematic of the experimental setup for pressure measurement applying PTV in the method 1. The laser was focused to a depth of 1.43 mm in distilled water by the objective lens. The distilled water contains 0.021 wt% the particulates (Sumitomo Seika Chemicals Co., Ltd., HE-3040, median diameter 9.4 μm, density 960 kg/m^3). To avoid interference between the particles, the size of the water tank was 153 mm × 215 mm × 36 mm. The motion of the particles was visualized by the He-Ne laser sheet light (NEC, GLG5700, wavelength 632.8 nm) and photographed by the CCD camera (Watec Co., Ltd., WAT-910HX, effective pixels 768 × 494, frame rate 29.97 fps, shutter speed 1/250 s) through the objective lens which was the same as focusing the femtosecond laser. The objective area was 75.6 μm × 50.5 μm, and depth of focus of the objective lens was 1.1 μm (at $\lambda = 550$ nm). Figure 6 shows a time chart of repetition frequency of the femtosecond laser and the frame rate of the CCD camera. Since the repetition frequency of the femtosecond laser was set to 10 Hz by the function generator, the three images were obtained when the shock wave was generated.

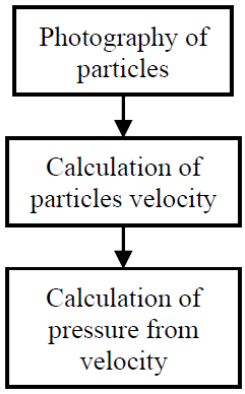

FIGURE 4. Flowchart of process to obtain shock pressure on method 1

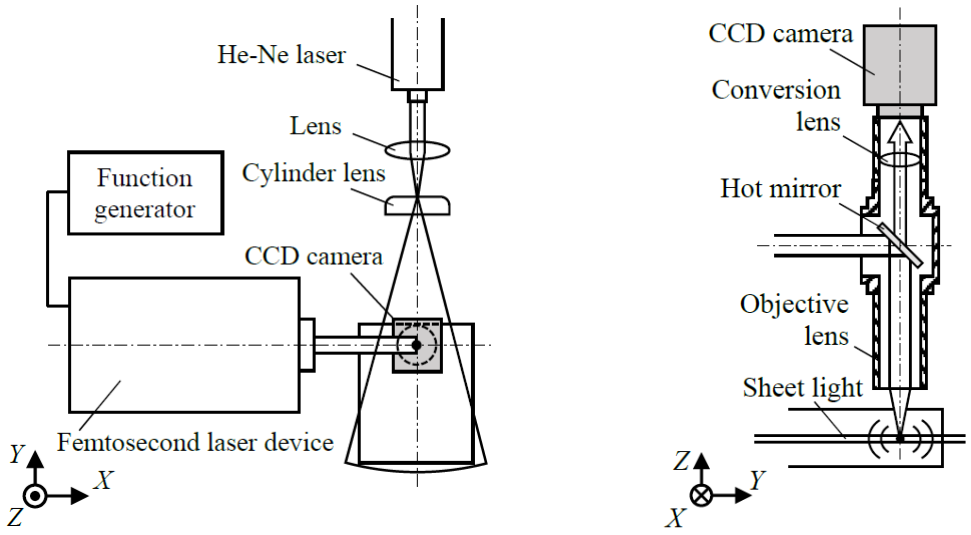

(a) Top view (b) Side view

FIGURE 5. Schematic of experimental setup for PTV

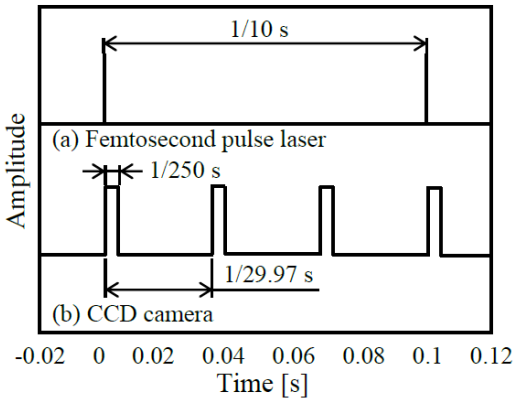

FIGURE 6. Time chart for repetition frequency of femtosecond laser and frame rate of CCD camera

3.2. **Analysis of velocity to pressure on method 1.**

3.2.1. *Equation of particles motion in water.* Figure 7 shows a conceptual diagram of particle movement by received shock waves in a one-dimensional region. The movement of a particle in a fluid can be expressed by using the following equation based on Newton's equation,

$$\rho_{\mathrm{s}} \frac{\pi}{6} d_{\mathrm{s}}^3 \frac{\mathrm{d}u_{\mathrm{s}}}{\mathrm{d}t} = F_{\mathrm{A}} + F_{\mathrm{D}} + F_{\mathrm{H}}, \tag{3}$$

where, left side of the equation is inertial force, ρ_{s} is density of particle, d_{s} is diameter of particle and u_{s} is velocity of particle. F_{A} is term about gradient of pressure and virtual mass, F_{D} is term of steady resistance by fluid and F_{H} is Basset term in right side of the equation. F_{A} is expressed as follows:

$$F_{\mathrm{A}} = \rho_{\mathrm{l}} \frac{\pi d_{\mathrm{s}}^3}{6} \left(\frac{\mathrm{D}u_{\mathrm{l}}}{\mathrm{D}t} \right) = \rho_{\mathrm{l}} \frac{\pi d_{\mathrm{s}}^3}{6} \left(\frac{1}{\rho_{\mathrm{l}}} \frac{\mathrm{d}p}{\mathrm{d}r} + K \right). \tag{4}$$

Moreover, F_{A} can be expressed by ignoring mass force K as follows:

$$F_{\mathrm{A}} = \frac{\pi d_{\mathrm{s}}^3}{6}\frac{\mathrm{d}p}{\mathrm{d}r}. \tag{5}$$

Next, F_{D} is expressed as follows:

$$F_{\mathrm{D}} = \frac{\pi d_{\mathrm{s}}^2}{8}\rho_{\mathrm{l}} C_{\mathrm{D}} |u_{\mathrm{l}} - u_{\mathrm{s}}|(u_{\mathrm{l}} - u_{\mathrm{s}}). \tag{6}$$

In Equation (6), C_{D} is expressed by Stokes law of drag,

$$C_{\mathrm{D}} = \frac{24}{\mathrm{Re}_{\mathrm{D}}}, \tag{7}$$

where, Re_{D} is particle Reynolds number,

$$\mathrm{Re}_{\mathrm{D}} = \frac{|u_{\mathrm{l}} - u_{\mathrm{s}}|}{\mu_{\mathrm{l}}}\rho_{\mathrm{l}} d_{\mathrm{s}}. \tag{8}$$

Therefore, Equation (6) can be transformed to the following equation:

$$F_{\mathrm{D}} = 3\pi d_{\mathrm{s}} \mu_{\mathrm{l}} (u_{\mathrm{l}} - u_{\mathrm{s}}). \tag{9}$$

From Equation (3), Equation (5) and Equation (9),

$$\frac{\mathrm{d}u_{\mathrm{s}}}{\mathrm{d}t} = \frac{1}{\rho_{\mathrm{s}}}\frac{\mathrm{d}p}{\mathrm{d}r} + 18\frac{\mu_{\mathrm{l}}}{d_{\mathrm{s}}^2 \rho_{\mathrm{s}}}(u_{\mathrm{l}} - u_{\mathrm{s}}). \tag{10}$$

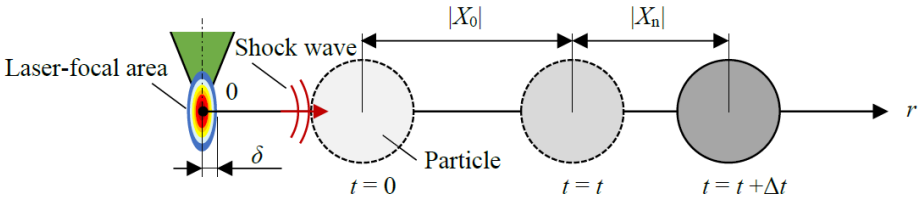

FIGURE 7. Conceptual diagram of particle movement by received shock waves in a one-dimensional region

(a) $t = 0$ (b) $t = \tau$

FIGURE 8. Schematic diagram of the relationship between the particle and the laser-focal area

Next, it is needed to explain that the change in the moving velocity of a particle received a shock wave. Figure 8 shows a schematic diagram of the relationship between the particle and the laser-focal area. In Equation (10), the received pressure can be expressed by the following equation based on the force balancing at each moment; when the shock wave acts on the particles ($t = 0$) and the particle begins to move ($t > 0$).

$$P(t) = \begin{cases} P_{\max}\left(\dfrac{\delta}{r}\right)^2 & (t = 0) \\ 0 & (t > 0) \end{cases}. \tag{11}$$

Because p is 0 when t is over 0, $\mathrm{d}p/\mathrm{d}r$ is fixed at 0. And assume that u_l is 0 due to the velocity of stationary fluid. Equation (10) is rearranged as follows:

$$\frac{\mathrm{d}u_\mathrm{s}}{\mathrm{d}t} = -18\frac{\mu_\mathrm{l}}{d_\mathrm{s}^2\rho_\mathrm{s}}u_\mathrm{s}. \tag{12}$$

From Equation (12), u_s is expressed as

$$u_\mathrm{s} = \mathrm{A}\exp\left(-18\frac{\mu_\mathrm{l}}{d_\mathrm{s}^2\rho_\mathrm{s}}t\right), \tag{13}$$

where, the velocity of the particle received a shock wave becomes maximum velocity $u_\mathrm{s,max}$ with delay time τ.

$$u_\mathrm{s,max} = \mathrm{A}\exp\left(-18\frac{\mu_\mathrm{l}}{d_\mathrm{s}^2\rho_\mathrm{s}}\tau_\mathrm{s}\right), \tag{14}$$

$$\mathrm{A} = \frac{u_\mathrm{s,max}}{\exp\left(-18\frac{\mu_\mathrm{l}}{d_\mathrm{s}^2\rho_\mathrm{s}}\tau_\mathrm{s}\right)}. \tag{15}$$

In reality, τ is considered sufficiently small,

$$\mathrm{A} = \lim_{\tau_\mathrm{s}\to 0}\frac{u_\mathrm{s,max}}{\exp\left(-18\frac{\mu_\mathrm{l}}{d_\mathrm{s}^2\rho_\mathrm{s}}\tau_\mathrm{s}\right)} = u_\mathrm{s,max}, \tag{16}$$

$$u_\mathrm{s} = u_\mathrm{s,max}\exp\left(-18\frac{\mu_\mathrm{l}}{d_\mathrm{s}^2\rho_\mathrm{s}}\tau_\mathrm{s}\right). \tag{17}$$

From described above, the moving velocity of particle changes exponentially. Equation (10) is transformed to the following equation by applying thickness of shock waves ($\Delta p/\sigma$) to the gradient of pressure $\mathrm{d}p/\mathrm{d}r$.

$$\frac{\mathrm{d}u_\mathrm{s}}{\mathrm{d}t} = \frac{1}{\rho_\mathrm{s}}\frac{\Delta p}{\sigma} + 18\frac{\mu_\mathrm{l}}{d_\mathrm{s}^2\rho_\mathrm{s}}(u_\mathrm{l} - u_\mathrm{s}). \tag{18}$$

Equation (18) is organized in terms of Δp.

$$\Delta p = \frac{\mathrm{d}u_\mathrm{s}}{\mathrm{d}t}\rho_\mathrm{s}\sigma - 18\frac{\mu_\mathrm{l}}{d_\mathrm{s}^2}(u_\mathrm{l} - u_\mathrm{s})\sigma. \tag{19}$$

Based on assumption that the particle accelerates from a state of rest with frame rate of the CCD camera (Δt), $\mathrm{d}u_\mathrm{s}/\mathrm{d}t$ becomes $u_\mathrm{s}/\Delta t$.

$$\Delta p = \frac{u_\mathrm{s}}{\Delta t}\rho_\mathrm{s}\sigma - 18\frac{\mu_\mathrm{l}}{d_\mathrm{s}^2}(u_\mathrm{l} - u_\mathrm{s})\sigma. \tag{20}$$

3.2.2. *Calculation of particles velocity as exponential.* In this section, it is explained that calculation of moving distance of particle $|X_\mathrm{n}|$ and particle velocity V_0 from two images. The motion of the particles is investigated by image analysis, and the pressure of the shock wave at the laser-focal area is obtained from the particle velocity. First, the moving distance of particle $|X_\mathrm{n}|$ is calculated from two images at time of t and $t + \Delta t$. In determining the particle velocity $|V_0|$ from the two distances $|X_0|$ and $|X_\mathrm{n}|$, it is considered that the distance also varies exponentially. Therefore, $|X_\mathrm{n}|$ is expressed by following equation with coefficient B.

$$|X_\mathrm{n}| = |X_0|\exp(-\mathrm{B}t), \tag{21}$$

$$\mathrm{B} = \frac{\ln|X_0| - \ln|X_\mathrm{n}|}{t}. \tag{22}$$

By differentiating Equation (21), the following equation is obtained.

$$|V_{\mathrm{n}}| = |V_0| \exp(-\mathrm{B}t) - \mathrm{B}|X_0| \exp(-\mathrm{B}t), \tag{23}$$

$$|V_0| = \frac{|X_{\mathrm{n}}|}{\exp(-\ln|X_0| + \ln|X_{\mathrm{n}}|)t} + \left(\frac{\ln|X_0| - \ln|X_{\mathrm{n}}|}{t}\right)|X_0|. \tag{24}$$

The received pressure of the particle ΔP is calculated by substituting $|V_0|$ for u_{s} in Equation (20). And the pressure at the laser-focal area is obtained by substituting ΔP for Equation (11) from relationship of the pressure and distance from the laser-focal area. In this calculation, density ρ_{l} was fixed at 998.2 kg/m^3, viscosity μ was fixed at 1.002 mPa·s and time t was determined to 33 ms from frame rate of the CCD camera.

In addition, the rise time t_{rise} and thickness σ of the shock waves is calculated as follows [21]:

$$t_{\mathrm{rise}} = \frac{P_{\max}}{(\mathrm{d}P/\mathrm{d}t)_{\max}}, \tag{25}$$

$$\sigma = ct_{\mathrm{rise}}, \tag{26}$$

where, $P_{\max}$ is the peak pressure, $(\mathrm{d}P/\mathrm{d}t)_{\max}$ is the maximum gradient of pressure and c is sound velocity of water. From Equation (25) and Equation (26), the rise time was obtained to 15.4 ns, and the thickness of the shock wave was obtained to 22.77 µm at r = 300 µm from Figure 2.

3.3. **Result on method 1.** Figure 9 shows received pressure of particles at each distance in method 1. The averaged pressure at the laser-focal area was calculated to be $P_{\max}$ = 28.92 MPa. However, the calculated pressure was very higher than the estimated pressure using the hydrophone (Section 2). The reason for the large difference was that the time determined from frame rate of the CCD camera was 33 ms and it was very longer than shock wave phenomena. It was considered that obtained velocity of particles may be terminal velocity. In addition, as the time became longer and the distance of movement, the required observation area also became larger. Therefore, there was possibility that the target of analysis may be mistakenly captured if a particle moves to out of the observation area. To improve pressure measurement applying PTV accuracy, it was necessary to shorten the time for shooting.

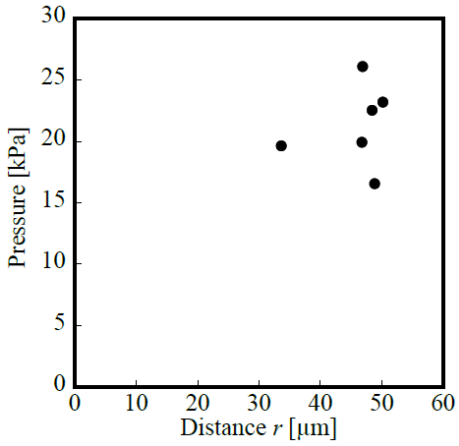

FIGURE 9. The pressure of the particle received by shock wave

4. Method 2 of Pressure Measurement Applying PTV.

4.1. Experimental setup for method 2. In this method, the time for shooting became shorter than method 1 by using the nano-pulse light with flash duration of nanosecond, and the pressure of shock waves was obtained from behavior of visualized particles. Figure 10 shows the flowchart of process to obtain shock wave pressure on method 2. As shown in Figure 10, the image analysis is conducted after photography of the moving particles received shock waves in the method 2. In addition, velocity and shock wave pressure are calculated. First, the experimental setup of method 2 is mentioned. Figure 11 shows a schematic of the experimental setup for particle visualization in method 2. The laser was focused to a depth of 1.43 mm in distilled water mixed particles. The particles close to the laser-focal area were visualized momentary by nano-pulse light (Sugawara Laboratories Inc., NP-1A/NPL-5, flash duration 180 ns) which was installed under the water tank. The observation area was the same as method 1, which was 75.6 μm × 50.5 μm and

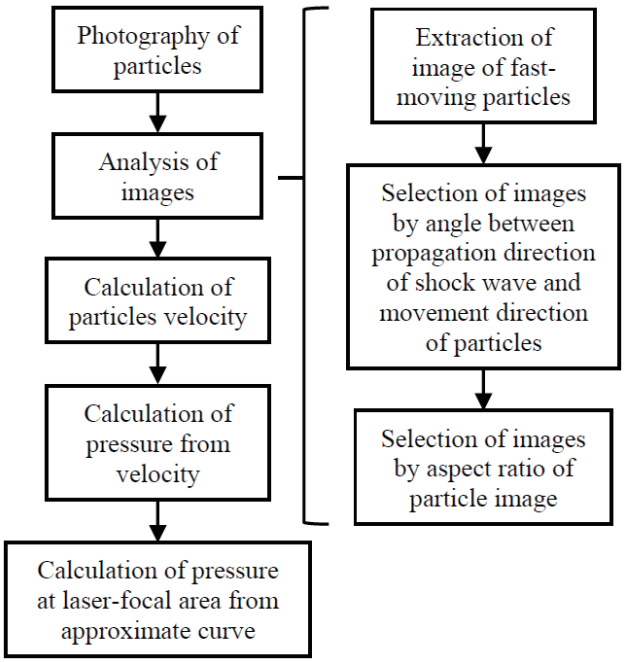

FIGURE 10. Flowchart of process to obtain shock pressure on method 2

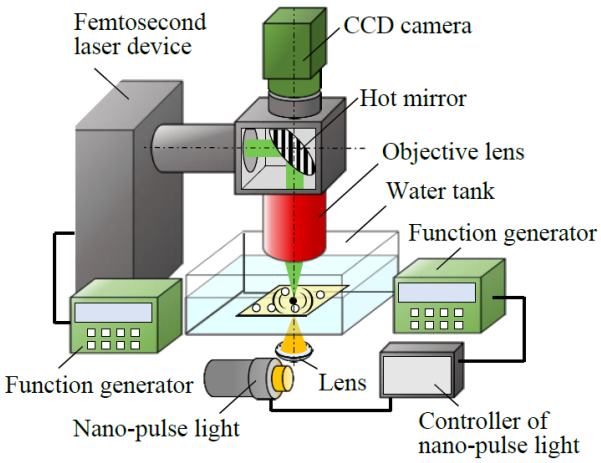

FIGURE 11. Experimental setup for the particle visualization

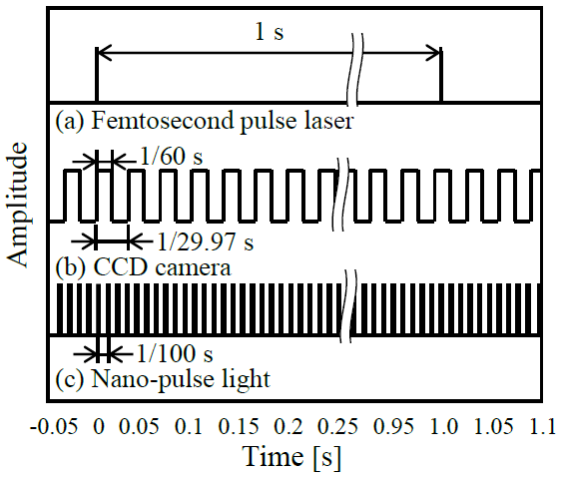

FIGURE 12. Time chart for repetition frequency of femtosecond laser, frame rate of CCD camera and repetition frequency of nano-pulse light

depth of focus of the objective lens was 1.1 μm. The repetition frequency of the laser and the frequency of flash of the nano-pulse light were set to 1 Hz and 100 Hz, respectively. Figure 12 shows a time chart of repetition frequency of the femtosecond laser, the frame rate of the CCD camera and the repetition frequency of the nano-pulse light.

4.2. **Procedure of selection particle pictures.** The particles are visualized only during time of flash duration of the light. The image (history) of the particles becomes perfectly circular because the particles are a state of rest or low-speed movement when the shock waves are not generated. Conversely, when a shock wave is generated, the image becomes elliptical due to receiving the shock wave and high-speed movement. In this experiment, to extract a particle which was anticipated to receive the shock waves by image analysis, the moving distance was obtained from major and minor axes of particles. Figure 13 shows a conceptual diagram of the calculation of moving distance in image analysis. Here, the time for movement of particle is determined to 180 ns from flash duration of the nano-pulse light. In this method, it was considered that the time is equally short compared to shock wave phenomena, the velocity and the moving distance decelerate linearly. The velocity V_0 is expressed as follows:

$$V_0 = \frac{|X_0|}{t}, \tag{27}$$

where $|X_0|$ is the moving distance of particles. In the case of assumed decelerating linearly, the velocity of the particle is high. Therefore, since Reynolds number is also high and

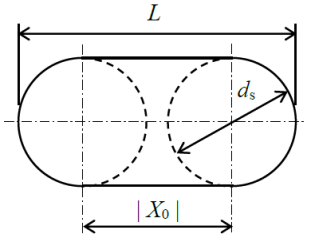

FIGURE 13. Particle motion after receiving a shock wave

Stokes law of drag cannot be applied, the drag coefficient is calculated by Schiller-Naumann equation ($\mathrm{Re_D} \leq 1000$),

$$C_\mathrm{D} = \frac{24}{\mathrm{Re_D}} \left(1 + 0.15\mathrm{Re_D^{0.687}}\right). \tag{28}$$

C_D is applied to Equation (6),

$$F_\mathrm{D} = 3\pi d_\mathrm{s}\mu_\mathrm{l}\frac{\rho_\mathrm{s}}{\rho_\mathrm{l}} \left(1 + 0.15\mathrm{Re_D^{0.687}}\right)(u_\mathrm{l} - u_\mathrm{s}). \tag{29}$$

Therefore, Equation (3) is transformed from Equation (5) and Equation (29),

$$\rho_\mathrm{s}\frac{\pi}{6}d_\mathrm{s}^3\frac{\mathrm{d}u_\mathrm{s}}{\mathrm{d}t} = \frac{\pi}{6}d_\mathrm{s}^3\frac{\mathrm{d}p}{\mathrm{d}r} + 3\pi d_\mathrm{s}\mu_\mathrm{l}\frac{\rho_\mathrm{s}}{\rho_\mathrm{l}} \left(1 + 0.15\mathrm{Re_D^{0.687}}\right)(u_\mathrm{l} - u_\mathrm{s}), \tag{30}$$

$$\frac{\mathrm{d}u_\mathrm{s}}{\mathrm{d}t} = \frac{1}{\rho_\mathrm{s}}\frac{\mathrm{d}p}{\mathrm{d}r} + 18\frac{\mu_\mathrm{l}}{d_\mathrm{s}^2\rho_\mathrm{l}} \left(1 + 0.15\mathrm{Re_D^{0.687}}\right)(u_\mathrm{l} - u_\mathrm{s}). \tag{31}$$

As above, $\mathrm{d}p/\mathrm{d}r$ becomes $\Delta p/\sigma$ based on the thickness of the shock waves,

$$\frac{\mathrm{d}u_\mathrm{s}}{\mathrm{d}t} = \frac{1}{\rho_\mathrm{s}}\frac{\Delta p}{\sigma} + 18\frac{\mu_\mathrm{l}}{d_\mathrm{s}^2\rho_\mathrm{l}} \left(1 + 0.15\mathrm{Re_D^{0.687}}\right)(u_\mathrm{l} - u_\mathrm{s}), \tag{32}$$

$$\Delta p = \frac{\mathrm{d}u_\mathrm{s}}{\mathrm{d}t}\rho_\mathrm{s}\sigma - 18\frac{\mu_\mathrm{l}}{d_\mathrm{s}^2\rho_\mathrm{l}}\rho_\mathrm{s}\sigma \left(1 + 0.15\mathrm{Re_D^{0.687}}\right)(u_\mathrm{l} - u_\mathrm{s}). \tag{33}$$

The received pressure of the particle Δp is calculated by substituting $|V_0|$ for u_s in Equation (33).

The pressure of shock waves decreases exponentially with increasing the propagation distance from the laser-focal area. The pressure at the laser-focal area was estimated by the received pressure of the particles at each distance and Equation (2). By substituting the theoretical radius of laser-focal area (1.257 μm) for r in Equation (2), pressure at the laser-focal area P_max was obtained. In the image analysis, the two threshold values were defined. The one of threshold value is angle between the vector from laser-focal area to particle (propagation direction of shock wave) and the vector in the direction of particle movement as shown in Figure 14. The other threshold value is aspect ratio L/d_s of particle image.

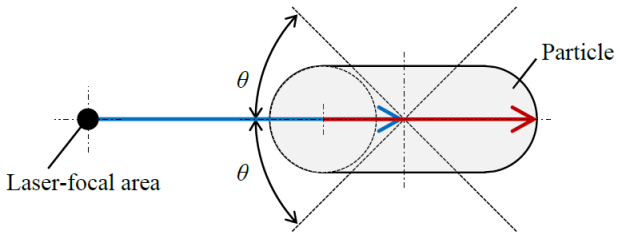

FIGURE 14. Angle between propagation direction of shock wave and movement direction of particle

4.3. **Result of PTV on method 2.** Figure 15 shows the relationship of the obtained angle and distance. Figure 16 shows the relationship of the obtained aspect ratio of the particle image and distance. From Figure 15, it was obtained that the value of angle was widely distributed at each distance. When all of the pressure of shock wave acts on the particle, the angle between two vectors should be close to 0°. However, many large angles were also obtained in this experiment. Where the distance from particles to the laser-focal area is closely, the radius of curvature of propagating spherical shock waves is smaller and

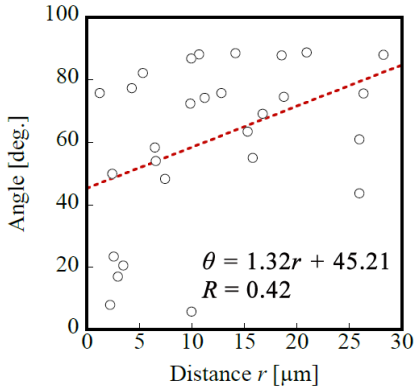

FIGURE 15. Relationship of the obtained angle and distance

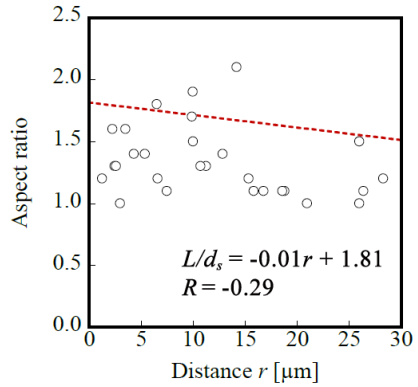

FIGURE 16. Relationship of the obtained aspect ratio of the particle image and distance

closer to the radius of curvature of the particle. Because probability of the shock wave and the particle hitting perpendicularly becomes low, it was considered that the particle moved to different directions with the direction of the propagating shock waves. Then, the particle images with the angle above 45° were removed in this calculation of pressure of the shock waves. In addition, to ignore the effect of particles which does not receive the shock waves perpendicularly and move in the direction of the water depth, the particle images with the aspect ratio below 1.3 were also removed from Figure 16. After this process, the pressure at the laser-focal area was attempted to calculate by applying the extrapolation (Equation (2)) to the received pressure of particles.

Figure 17 shows the relationship between received pressure of particles and distance. From Figure 17, the pressure at laser-focal area was estimated to be 7.02 MPa by applying the extrapolation which indicated dot line. This value was the same order as the result obtained by the hydrophone (Section 2). There was possibility that pressure measurement applying PTV is applicable to the shock wave phenomena. However, as an absolute value was twice as different, and the gradient of the extrapolation was 0.142 which was lower than the gradient obtained by the hydrophone. The gradient of approximate curve of the measurement with hydrophone was 0.416, and it was indicated that the pressure decay was more gradually in the method. For the reason, it was considered that the number of data points has been reduced due to two thresholds, and the obtained particle images were limited to distance of 10 μm or less from the laser-focal area. Furthermore, another factor may be that the rise time and the thickness of the shock wave were determined from pressure history at $r = 300$ μm in this research. In reality, since the shape and

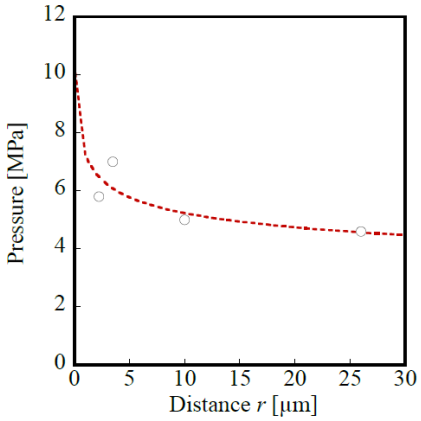

FIGURE 17. Relationship between received pressure of particles and distance

developmental status have not been elucidated at $r = 300$ μm, the using shock wave characteristics such as rise time and thickness might not be appropriate to calculate the received pressure of particles. Therefore, it is required to increase the number of data and investigate the shape of the shock wave, etc. for establishment of the pressure measurement applying PTV.

5. **Conclusions.** This research proposed methods applying particle tracking velocimetry as the measurement for the micro shock waves.

1) The pressure histories were obtained by measurement using hydrophone in the distance from 300 μm to 1000 μm from laser-focal area. It was confirmed that the peak pressure was approximately 0.4 MPa at 300 μm. The pressure at the laser-focal area was estimated to be 3.70 MPa by the extrapolation.

2) The method of pressure measurement was proposed, which can measure at the laser-focal area applying PTV. Assuming that velocity of the particle received the shock waves decreases exponentially in time determined from frame rate from CCD camera, the pressure at the laser-focal area was estimated to be 28.92 MPa. The pressure was very higher than the estimated value by using hydrophone because the frame rate was millisecond order which may be longer than shock wave phenomena.

3) By using nano-pulse light for illumination, the time interval of moving particles was shortened to nanosecond order, and the pressure was calculated assuming that the particle velocity varies linearly. The pressure at the laser-focal area was estimated to be 7.02 MPa, which was the same order as the estimated value by using hydrophone. From the result, there was possibility that the pressure measurement applying PTV is applicable to the shock wave phenomena. However, the experimental result was used for this calculation, and the shape of the shock waves has not been elucidated.

Acknowledgment. A part of this work was supported by Grant-in-Aid for Scientific Research (B) 21H01252 and a Grant-in-Aid for JSPS Fellows 23KJ1752. The authors wish to thank R. Sakai, R. Terajima who assisted with data collection for this study.

REFERENCES

[1] S. Sundaram, K. Sellamuthu, K. Nagavelu, H. R. Suma, A. Das, R. Narayan, D. Chakravortty, J. Gopalan and S. M. Eswarappa, Stimulation of angiogenesis using single-pulse low-pressure shock wave treatment, *Journal of Molecular Medicine*, vol.96, pp.1177-1187, 2018.

[2] T. Takahashi, K. Nakagawa, S. Tada and A. Tsukamoto, Low-energy shock waves evoke intracellular Ca^{2+} increases independently of sonoporation, *Scientific Reports*, vol.9, 3218, 2019.

[3] R. Obana, A. Yamamoto and M. Tamagawa, Effects of underwater plane shock waves on neutrophil propulsion, *Journal of Biomechanical Science and Engineering*, vol.17, no.3, pp.1-12, 2022.
[4] Y.-E. Kuo, C.-C. Wu, Y. Hosokawa, Y. Maezawa, K. Okano, H. Masuhara and F.-J. Kao, Local stimulation of cultured myocyte cells by femtosecond laser-induced stress wave, *Appl. Phys. A*, vol.101, pp.597-600, 2010.
[5] V. G. Godinez, V. Morar, C. Carmona, Y. Gu, K. Sung, L. Z. Shi, C. Wu, D. Preece and M. W. Berns, Laser-induced shockwave (LIS) to study neuronal Ca^{2+} responses, *Frontiers in Bioengineering and Biotechnology*, vol.9, 598896, 2021.
[6] S. Seno, S. Tomura, H. Miyazaki, S. Sato and D. Saitoh, Effects of selective serotonin reuptake inhibitors on depression-like behavior in a laser-induced shock wave model, *Front. Neurol.*, vol.12, 602038, 2021.
[7] S. Norio, T. Kazuyoshi and I. Jun, An experimental study of the behavior of bubbles and shock waves generated by laser focusing in water, *Transactions of the Japan Society of Mechanical Engineers Series B*, vol.53, no.486, pp.317-325, 1987.
[8] T. Yasuda, N. Takahashi, M. Baba, K. Tei and S. Yamaguchi, An experimental study on micro-bubble generation by laser-induced breakdown in water, *The Review of Laser Engineering Supplemental*, vol.2008, pp.1273-1275, 2008.
[9] K. Hayasaka, Y. Tagawa, T. Liu and M. Kameda, Optical-flow-based background-oriented schlieren technique for measuring a laser-induced underwater shock wave, *Experiments in Fluids*, vol.57, pp.1-11, 2016.
[10] Y. Tagawa, S. Yamamoto, K. Hayasaka and M. Kameda, On pressure impulse of a laser-induced underwater shock wave, *J. Fluid Mech.*, vol.808, pp.5-18, 2016.
[11] A. Vogel and W. Lauterborn, Acoustic transient generation by laser-produced cavitation bubbles near solid boundaries, *J. Acoust. Soc. Am.*, vol.84, no.2, pp.719-731, 1988.
[12] A. Vogel, S. Busch and U. Parlitz, Shock wave emission and cavitation bubble generation by picosecond and nanosecond optical breakdown in water, *J. Acoust. Soc. Am.*, vol.100, no.1, pp.148-165, 1996.
[13] A. Vogel, J. Noack, K. Nahen, D. Theisen, S. Busch, U. Parlitz, D. X. Hammer, G. D. Noojin, B. A. Rockwell and R. Birngruber, Energy balance of optical breakdown in water at nanosecond to femtosecond time scales, *Appl. Phys. B*, vol.68, pp.271-280, 1999.
[14] V. Venugopalan, A. Guerra, III, K. Nahen and A. Vogel, Role of laser-induced plasma formation in pulsed cellular microsurgery and micromanipulation, *Phys. Rev. Lett.*, vol.88, no.7, 2002.
[15] A. Vogel, J. Noack, G. Hüttman and G. Paltauf, Mechanisms of femtosecond laser nanosurgery of cells and tissues, *Appl. Phys. B*, vol.81, pp.1015-1047, 2005.
[16] W. Lauterborn and A. Vogel, Shock wave emission by laser generated bubbles, in *Bubble Dynamics and Shock Waves. Shock Wave Science and Technology Reference Library*, C. F. Delale (ed.), Berlin, Heidelberg, Springer, 2013.
[17] Y. Hosokawa, H. Takabayashi, S. Miura, C. Shukunami, Y. Hiraki and H. Masuhara, Nondestructive isolation of single cultured animal cells by femtosecond laser-induced shockwave, *Appl. Phys. A*, vol.79, pp.795-798, 2004.
[18] T. Iino and Y. Hosokawa, Direct measurement of femtosecond laser impulse in water by atomic force microscopy, *Applied Physics Express*, vol.3, 107002, 2010.
[19] J. Sakai, D. Roldán, K. Ueno, H. Misawa, Y. Hosokawa, T. Iino, S. Wakitani and M. Takagi, Effect of the distance between adherent mesenchymal STEM cell and the focus of irradiation of femtosecond laser on cell replication capacity, *Cytotechnology*, vol.64, pp.323-329, 2012.
[20] T. Iino, P.-L. Li, W.-Z. Wang, J.-H. Deng, Y.-C. Lu, F.-J. Kao and Y. Hosokawa, Contribution of stress wave and cavitation bubble in evaluation of cell-cell adhesion by femtosecond laser-induced impulse, *Appl. Phys. A*, vol.117, pp.389-393, 2014.
[21] M. Tamagawa, T. Akamatsu, H. Watanabe, M. Uchida and Y. Imaide, Effects on living tissues induced by shock waves: 1st report, development of shock tube generating single pulse pressure wave for bio-test and animal experiments, *Transactions of the Japan Society of Mechanical Engineers Series B*, vol.60, no.579, pp.3762-3767, 1994.

Author Biography

Ayumu Yamamoto obtained his Ph.D. degree in Engineering from Kyushu Institute of Technology, Japan in 2024. He is currently a researcher in fluid mechanics at a mechanical manufacturer. His main research interest is the generation, measurement, and photography of laser-induced underwater micro shock waves.

Masaaki Tamagawa obtained his Ph.D. degree in Engineering from Kyoto University, Japan in 1996. He is currently a full-time professor at Kyushu Institute of Technology, Japan. His main research interests include fluid engineering, biomedical engineering, shock wave, CFD (computational fluid dynamics), drug delivery systems, regenerative medicine, micromachine, Thrombus, artificial organs, blood flows and mechanical engineering.